

## Supplementary Files to:

### Effects of FGFR inhibitors TKI258, BGJ398 and AZD4547 on breast cancer cells in 2D, 3D and tissue explant cultures

Kähkönen TE<sup>1</sup>, Toriseva M<sup>1,2</sup>, Petruk N<sup>1,2</sup>, Virta A-R<sup>1</sup>, Maher A<sup>1</sup>, Eigélienė N<sup>1</sup>, Kaivola J<sup>1</sup>, Boström P<sup>3</sup>, Koskivuo I<sup>4</sup>, Nees M<sup>1,5</sup>, Tuomela JM<sup>1,2</sup>, Ivaska KK<sup>1</sup> and Härkönen PL<sup>1,2</sup>.

<sup>1</sup> University of Turku, Institute of Biomedicine, 20520 Turku, Finland

<sup>2</sup> FICAN West Cancer Centre, Turku, 20520 Turku, Finland

<sup>3</sup> Turku University Hospital, Department of Pathology, 20520 Turku, Finland

<sup>4</sup> Turku University Hospital, Department of Plastic and General Surgery, 20520 Turku, Finland

<sup>5</sup> Uniwersytet Medyczny w Lublinie, Dept. of Biomedicine and Molecular Biology II, 20-095 Lublin, Poland

#### Corresponding author:

Pirkko Härkönen, Institute of Biomedicine, University of Turku, Kiinamylynkatu 10, 20520 Turku, Finland, Email: [harkonen@utu.fi](mailto:harkonen@utu.fi)

**Supplementary Table S1.**

**FGFRis used in the study.** The IC<sub>50</sub> values (nM) for the non-selective FGFRi TKI258 and the FGFR selective inhibitors BGJ398 and AZD4547. The dash symbol (‘ - ‘) refers to no binding to the receptor. The IC<sub>50</sub> values are summarized in the following publications: [5] Katoh 2016, [7] Katoh and Nagama 2014, [20] Babina and Turner 2017.

<b>Inhibitor</b>	<b>IC<sub>50</sub> (nM)</b>					<b>References</b>
	<b>FGFR1</b>	<b>FGFR2</b>	<b>FGFR3</b>	<b>FGFR4</b>	<b>Other targets</b>	
<b>TKI258</b>	8	40	9	-	VEGFR1 (10 nM), VEGFR2 (13 nM), VEGFR3 (8 nM), Kit (2 nM), CSF1R (36 nM), FLT3 (1 nM), PDGFRA (~200 nM), PDGFRB (27 nM)	Katoh and Nagama 2014 Katoh 2016 Babina and Turner 2017
<b>BGJ398</b>	0.9	1.4	1	60	-	Katoh 2016
<b>AZD4547</b>	0.2	1.8	2.5	165	VEGFR2 (24 nM), Kit (24 nM), CSF1R (9.7 nM), FLT3 (85 nM), IGFR (518 nM)	Katoh and Nagama 2014 Katoh 2016 Babina and Turner 2017

**Supplementary Table S2.****Primer sequences and information about primary and secondary antibodies used in the study.**

<b>Gene</b>	<b>Forward primer sequence</b>	<b>Reverse primer sequence</b>
FGFR1	5'-TGG CAC CCG AGG CAT TAT TT-3'	5'-CAT GTA CAG CTG GTT GTT GC-3'
FGFR2	5'-AAC AGT CAT CCT GTG CCG AA-3'	5'-AGC CGA AAC TGT TAC CTG TC-3'
FGFR3	5'-CGT CCA CCG ACG AGT ACC T-3'	5'-CTC ACA TTG TTG GGG ACC AGT-3'
FGFR4	5'-CTG ACA CAG TGC TCG ACC TT-3'	5'-AAC CCT GAC ATT TGG GCC AT-3'
beta-actin	5'-CGT GGG GCG CCC CAG' GCA CCA-3	5'-TTG GCC TTG GGG TTC AGG GGG-3'

<b>Antibody</b>	<b>Manufacturer</b>
phospho-FRS2	Cell Signaling Technologies, #3864
phospho-ERK1/2	Cell Signaling Technologies, #4370
total-ERK1/2	Cell Signaling Technologies, #9101
alpha-tubulin	Abcam, ab4074
Anti-rabbit 800CW	Li-Cor, 925-32213
Anti-mouse 680RD	Li-Cor, 925-68072
HRP-conjugated anti-rabbit	Abcam, ab6721
Anti-FGFR1	Abcam, ab10646
Anti-FGFR2	Abcam, ab10648
Anti-FGFR3	Santa Cruz, sc-13121
Anti-FGFR4	Santa Cruz, sc-124

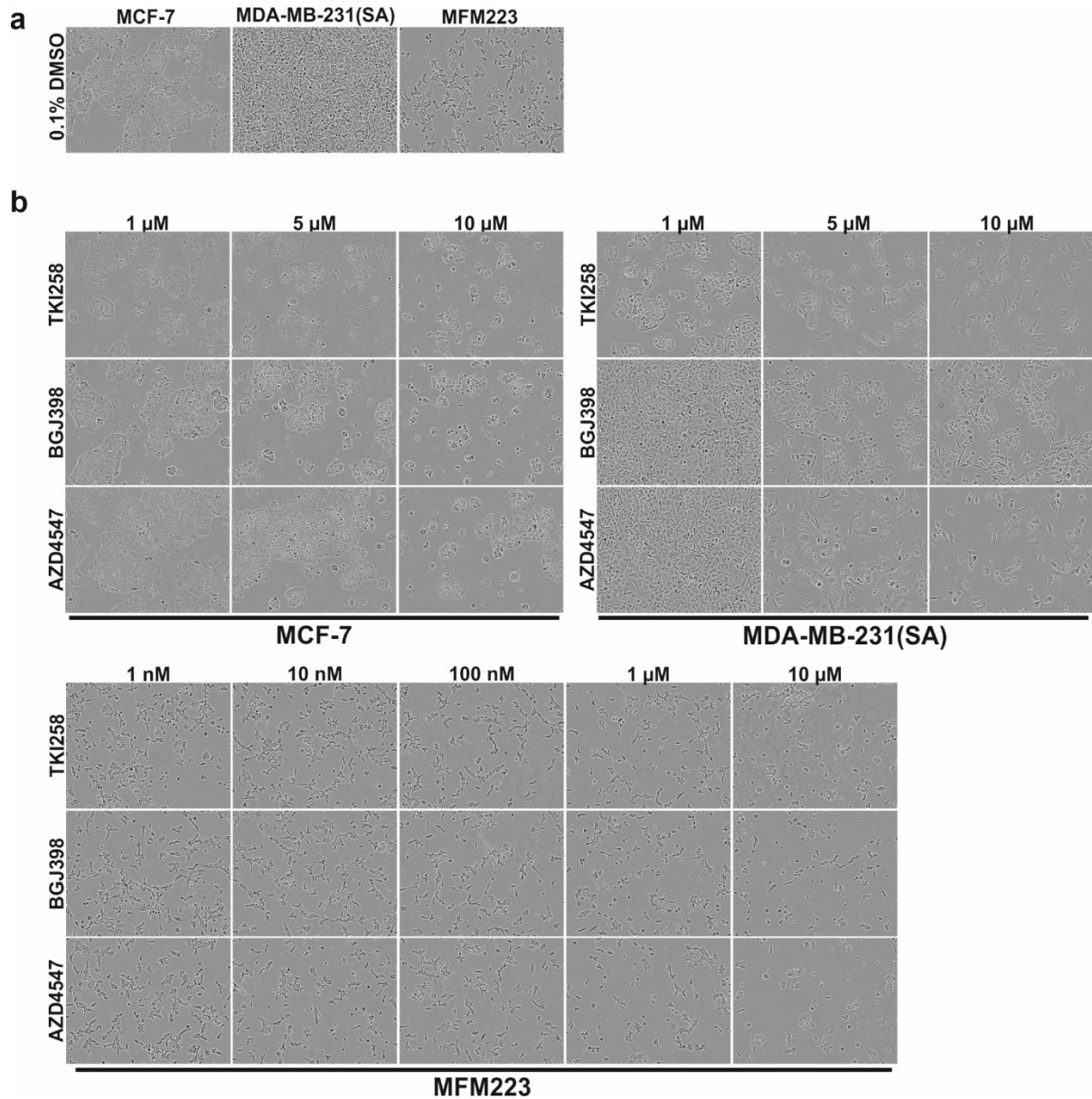
**Supplementary Table S3.**

**Patient information and tumor characteristics.** Classification of the tumor samples by a pathologist. The data includes artificial patient ID, age, cancer type and grade, lymph node status, observed metastasis (yes/no), and ER (%), PR (%), HER2 (yes/no) expression, and results from Ki67 staining (%) at tumor dissection by a clinical pathologist.

<b>Patient ID</b>	<b>Tumor classification</b>				<b>Expression in tumor</b>			
	<b>Type</b>	<b>Gradius</b>	<b>Nodes</b>	<b>Metastasis</b>	<b>ER (%)</b>	<b>PR (%)</b>	<b>HER2</b>	<b>Ki67 (%)</b>
<b>1</b>	Ductal	3	0	No	70	95	No	65
<b>2</b>	Ductal	3	2/50	Yes	90	90	No	9
<b>3</b>	Ductal	2	0/12	No	99	95	No	30
<b>4</b>	Lobular	2	29/35	Yes	98	98	No	30
<b>5</b>	Ductal	2	3/27	Yes	95	20	Yes	9
<b>6</b>	Ductal	2	3/15	Yes	90	98	Yes	30
<b>7</b>	Ductal	2	3/8	Yes	98	98	No	30
<b>8</b>	Lobular	2	0/8	No	99	95	No	15
<b>9</b>	Lobular	2	0/8	No	95	45	No	29
<b>10</b>	Lobular	2	0/8	No	98	95	No	12

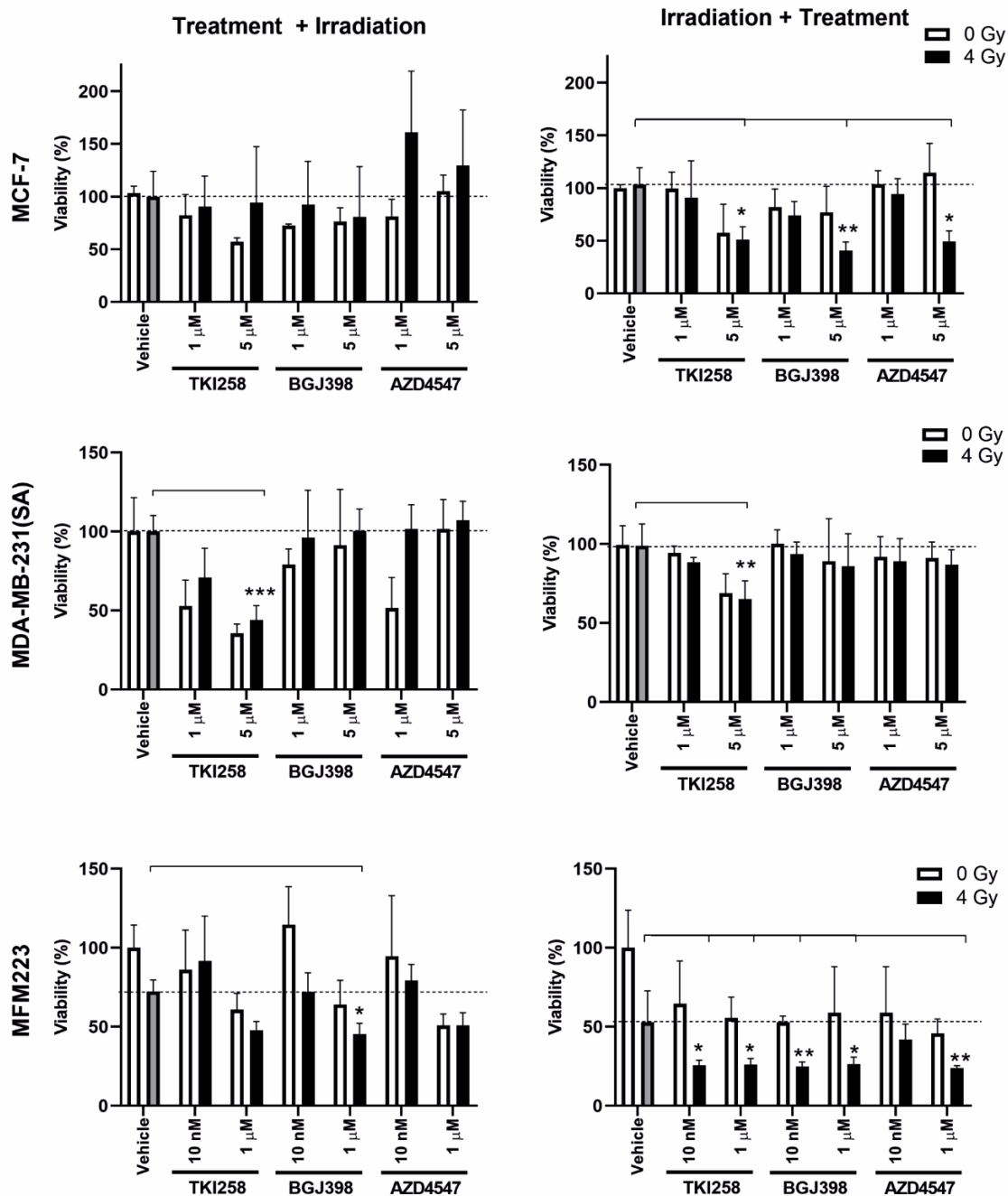
### Supplementary Figure S1.

**MCF-7, MDA-MB-231(SA), and MFM223 cells treated with TKI258, BGJ398, and AZD4547.** MCF-7, MDA-MB-231(SA) and MFM223 cells were treated with TKI258, BGJ398 and AZD4547 at the indicated concentrations for 70 h. IncuCyte ZOOM microscope imaging was used to monitor cell proliferation in real-time and representative images at the 70 h point are shown.



## Supplementary Figure S2.

**Combination of FGFRis with irradiation.** MCF-7 or MDA-MB-231(SA) cells (2000/well) were treated with 1 or 5  $\mu$ M, and MFM223 cells (10000/well) with 10 nM or 1  $\mu$ M of FGFRis for 24 h and then irradiated with 0 or 4 Gy X-ray. Medium was changed to FGFRi-free medium after 24 h, and cell viability measured 48 h later (left). Alternatively, cells were first irradiated with 0 or 4 Gy of X-ray and the treatment with FGFRis was started 48 h after irradiation. Medium was changed to FGFRi-free medium after 24 h, and cell viability measured 48h later (right). Cell viability (% of untreated control, mean  $\pm$  SD, n=3-4) after each treatment in non-irradiated (0 Gy, white bars) and irradiated (4 Gy, black bars) cells. Cells exposed to both FGFRi and irradiation (black) were compared to the vehicle-treated cells exposed to irradiation alone (gray bars, dotted line). Statistical significances are shown for One-Way ANOVA, with Dunnett's test for multiple comparison ( $p < 0.05^*$ ,  $p < 0.01^{**}$ ,  $p < 0.001^{***}$ ).



### Supplementary Figure S3.

**Confocal imaging of organotypic 3D cultures and the morphometric image analysis.** A) At the endpoint of cultures, organotypic 3D cultures were stained with Calcein-AM (green) and EthD1 (red) to visualize live and dead cells in organoids, respectively. The organoids were imaged with a confocal microscope with 5x objective, and representative images are shown. B) Maximum projections were segmented and analyzed using AMIDA-software. Example images of the segmentations are shown.

